SCIENTIFIC REPORTS

明胶-鞣酸多层包覆型一氧化氮气体输送系统的调控性能研究

OPEN

Developing regulatory property of gelatin-tannic acid multilayer films for coating-based nitric oxide gas delivery system

Received: 19 December 2018
Accepted: 9 May 2019
Published online: 05 June 2019

为了利用一氧化氮气体在抗菌、抗癌、伤口愈合应用中的潜力，在过去几十年中进行了许多研究来开发NO传递系统。虽然涂层方法和flm类型对于应用于以前NO输送系统的生物医学设备涂层是必不可少的，但从涂层系统中释放控制仍然具有挑战性。

在本研究中，我们引入了一种多层聚合物涂层系统，以克服FLM系统不可控的NO释放动力学。我们利用生物相容性明胶和单宁酸构建了一种基于逐层自组装方法的粗糙、多孔结构FLM。多层聚合物结构促进了（Gel/TA）nflm的NO释放量的控制，并在早期表现出爆发释放。

我们通过高压NO气体下的化学反应，将质子反应的NO供体N-天顶酸（NONOates）合成（Gel/TA）n FLM。采用实时NO分析机（NOA280i）对NO释放曲线进行分析。然后，对NO释放（Gel/TA）n FLM对人真皮成纤维细胞的毒性和对金黄色葡萄球菌的杀菌作用进行了试验。

Kyungtae Park[1], Hyejoong Jeong[1], Junjira Tanum[1], Jae-chan Yoo[2] & Jinkee Hong[1]

To utilize potentials of nitric oxide (NO) gas in anti-bacterial, anticancer, wound healing applications, numerous studies have been conducted to develop a NO delivery system in the past few decades. Even though a coating method and film types are essential to apply in biomedical device coating from previous NO delivery systems, release control from the coating system is still challenging. In this study, we introduced a multilayered polymeric coating system to overcome the uncontrollable NO release kinetics of film systems. We used biocompatible gelatin and tannic acid to construct a rough, porous structured film based on the layer-by-layer self-assembly method. The multilayered polymeric structure facilitated the controlled amount of NO release from (Gel/TA)$_n$ film and showed burst release in early period owing to their large surface area from the rough, porous structure. We synthesized the proton-responsive NO donor, *N*-diazeniumdiolate (NONOates), into the (Gel/TA)$_n$ film through a chemical reaction under high pressure NO gas. NO release profile was analyzed by a real-time NO analysis machine (NOA 280i). Then, the NO-releasing (Gel/TA)$_n$ film was tested its toxicity against human dermal fibroblast cells and bactericidal effects against *Staphylococcus aureus*.

Nitric oxide (NO) is an endogenously produced gas molecule from L-arginine by three nitric oxide synthase (NOS) enzymes in the human body[1,2]. Since the NO gas was verified as a signaling molecule involved in many physiological and pathological processes such as angiogenesis[3–5], immune response[6,7], neurotransmission[8,9], and antibacterial effect[10,11], many studies have been conducted to develop NO gas delivery systems for biomedical applications. The function of NO in the human body highly depends on its concentration, however, its unstable property makes it difficult to develop a controlled NO delivery system. Therefore, recent studies have focused on developing a controlled release NO delivery system to take advantages of the helpful effect of NO gas in the human body. From this perspective, various types of systems have been reported such as nanoparticles, small molecules that rapidly generate NO, liposomes, the polymer itself, hydrogel, and films[11–15]. Particularly, to apply NO delivery systems in biomedical devices, it is essential to develop a coating or a film system for NO delivery. In previous studies, the sol-gel reaction based coating, self-assembled monolayer, and simple adsorption onto surfaces have been studied as coating systems[14]. However, it is a still challenging to construct a coating system for controlled NO release.

To overcome the limitation of NO delivery coating, we designed the multilayered thin film with a precisely controllable NO donor amount via layer-by-layer (LbL) self-assembly. LbL self-assembly is one of the most widely studied thin film fabrication method because of its versatile process, outstanding properties of controlled drug release and gas capturing, sensing ability[16–20]. LbL technique, as a surface coating method, also can be applied to many types of substrates regardless of the material, shape, and size. Additionally, numerous materials can be used to construct building blocks such as graphene oxide, polypeptides, natural polymers, and synthetic polymers[21–27]. Therefore, it can be an appropriate method with biocompatible materials to apply for biomedical coatings.

Gelatin (Gel) is a natural protein that is highly biocompatible, shows good film-forming ability, and has wide applications in drug delivery, tissue engineering, and hydrogel studies. Gel also has many functional groups

[1]School of Chemical & Biomolecular Engineering, Yonsei University, 50 Yonsei Ro, Seodaemun Gu, Seoul, 03722, Republic of Korea. [2]Biotechnology Research Center, JCBIO Co., LTD & Avison Biomedical Research Center (ABMRC), Yonsei University, Seoul, 03722, Republic of Korea. Correspondence and requests for materials should be addressed to J.H. (email: jinkee.hong@yonsei.ac.kr)

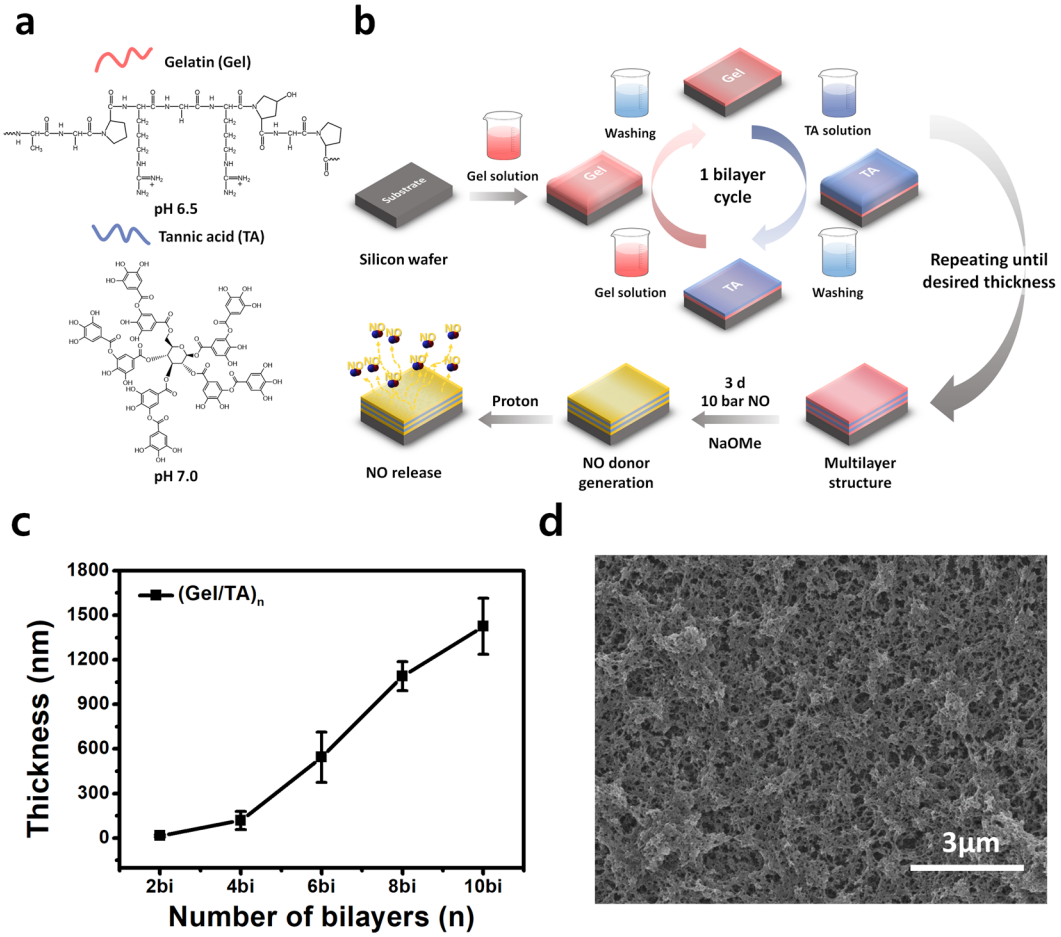

Figure 1. (**a**) Molecular structure and pH condition of film combination and (**b**) schematic illustration about preparation method of gelatin/tannic acid multilayer film for controlled nitric oxide release (**c**) film growth curve measured by profilometry and (**d**) scanning electron microscopy image of 10-bilayer film (Fig. 1 schematic illustration was drawn by K.P.).

that can participate in multiple interactions such as proline and 4-hydroxyproline for hydrophobic interactions, hydrogen bonding, and electrostatic interactions[28]. On the other hand, tannic acid (TA) is a natural polyphenol that can be extracted from plants, thus it is very biocompatible and has been studied for using in many biomedical applications. Additionally, tannic acid has many phenol groups that can bind with proteins through hydrophobic interactions and hydrogen bonding. Because of their biocompatibility and good film-forming property, many studies have been conducted to construct polymeric structures with gelatin and tannic acid[29–31].

Herein, we used natural materials Gel and TA that emphasized their biocompatible properties in the previous paragraph to develop a polymer-based coating system to improve the controlled release ability of NO delivery by constructing gelatin and tannic acid multilayer $(Gel/TA)_{n.}$(here, n means number of bilayers). We verified the assumption that the film with a roughness, porous structure enabled burst release of NO gas and burst release of NO can have bactericidal effects. We fabricated the multilayer film using the LbL self-assembly technique with different numbers of bilayers, then analyzed the film characteristics measuring the thickness growth tendency and the surface morphology. We confirmed NO donor formation by UV-vis spectrometry and analyzed NO release using a real-time chemiluminescence-based NO analysis device. We tested the applicability of the $(Gel/TA)_n$ film for biomedical applications via testing toxicity and antibacterial effects against human dermal fibroblast cells (HDF) and *Staphylococcus aureus* (*S. aureus*) which is commonly isolated species in chronic wound via skin infection[32,33].

Results and Discussion

Film growth and characteristics. We fabricated the $(Gel/TA)_n$ film by the well-known LbL self-assembly method as described in Fig. 1. We attempted to construct the films based on not only hydrophobic interaction, hydrogen bonding but also electrostatic interactions between the neighboring layers to achieve reproducible results. We set the pH value of the Gel solution at 6.5 below its pI value (pH 7–9)[34] and pH value of TA at 7.0 above its pKa value[29,35] to induce the ionization of each material for electrostatic interaction. We evaluated film thickness as the number of bilayers increased shown in Fig. 1. The thicknesses of films with 4 bilayers and 10 bilayers were 118.5 nm ± 61.2 nm and 1425.6 nm ± 188.5 nm, respectively. From the thickness results of the film increased regularly with linear growth tendency, we determined the $(Gel/TA)_n$ film was successfully constructed

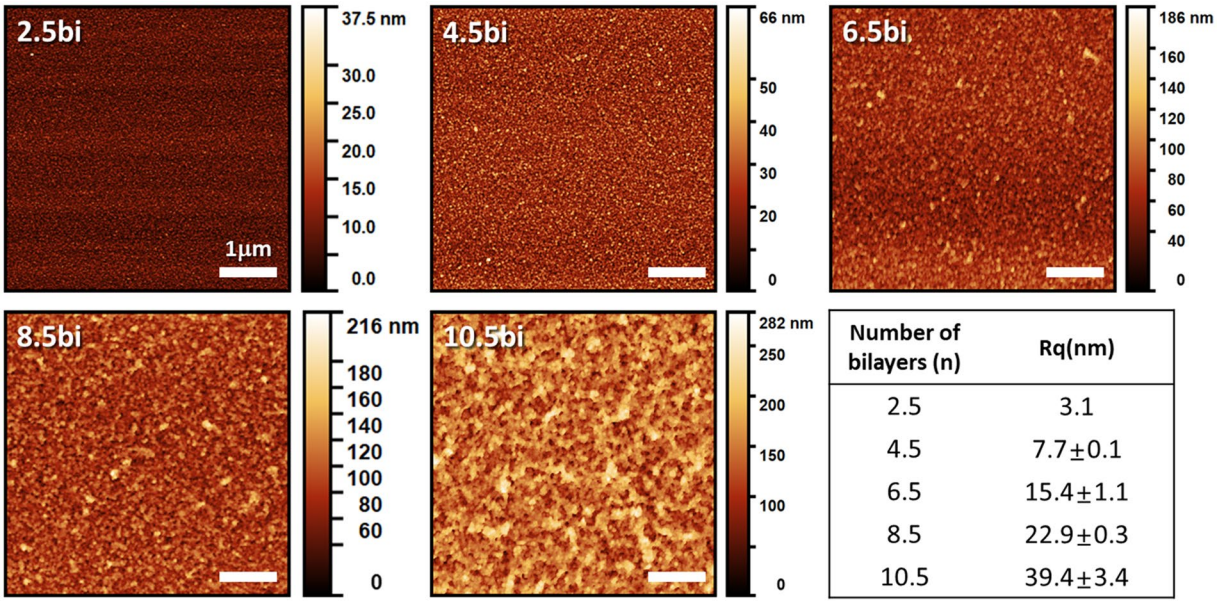

Number of bilayers (n)	Rq(nm)
2.5	3.1
4.5	7.7±0.1
6.5	15.4±1.1
8.5	22.9±0.3
10.5	39.4±3.4

Figure 2. Surface morphology of each film with different numbers of bilayers analyzed by atomic force microscopy.

by LbL assembly. In addition, an approximately 220-nm increase per bilayer was observed from 4 bilayers to 10 bilayers, indicating that the bulk film was constructed. According to many previous studies, the gelatin/polyphenol interaction is based on hydrogen bonding, hydrophobic interactions, and electrostatic interactions[29,35–37]. As the multiple binding sites between the protein and the tannic acid exist, the $(Gel/TA)_n$ film could diffuse into the neighboring layer during the LbL process[31]. Thus, the drastic increase was valid result considering those multiple interactions and diffusion. The porous and rough structure of the $(Gel/TA)_n$ film was confirmed from the SEM images shown in Fig. 1d (also see Supplementary Fig. 2) and it is corresponding to the topological images of the film measured by AFM shown in Fig. 2. The porous structure might be formed by a hydrophobic pocket between the hydrophobic side chain of gelatin and aromatic rings of TA, which was stabilized by hydrogen bonding[28]. We measured the root mean square roughness (Rq) using the AFM analysis program as well. Figure 2 shows the increasing tendency of surface roughness with film growth. The 10.5 bilayer film showed 39.4 ± 3.4 nm Rq roughness, which is 10-fold higher than that of the 2.5 bilayer film (3.1 nm). From the film growth data and the surface morphology, we determined that the $(Gel/TA)_n$ film could be successfully constructed at the certain pH condition and porous structure attributed to the exponential increase. Additionally, we assumed the porous structure and exponential increase of thickness would promote the NO donor generation and their release kinetics.

Roughness-dependent *N*-diazeniumdiolates (NONOates) synthesis in the Gel/TA film. We selected *N*-diazeniumdiolates (NONOates) as a NO-generating moiety for incorporation into the multilayer film among the many types of NO donor because of a proton-triggered generating mechanism producing two molecules of NO continuously in the physiological condition[32]. We simply synthesized the NO donor into the $(Gel/TA)_n$ film following the previous works. The synthesis process was carried out under the high pressure of NO gas, called high pressure reaction (HPR), to incorporate the NO donor into the $(Gel/TA)_n$ films forming the NONOates group at the amine group and amide bond sites of the Gel structure[38,39]. In this chemical reaction, NO gas reacted with the deprotonated amine site. From these reason, we added the sodium methoxide (NaOMe) for promoting deprotonation of the amine group as a catalyst. And it promotes the attack of NO gas into the deprotonated amine and amine groups[39–41]. We measured the film before and after the HPR by UV-vis absorbance to compare the amount of NO donor formation depending on the number of bilayers and its roughness. We hypothesized that the rough, porous structure would make a higher surface area, and cause the proportional increase result of NO donor formation to the thickness. Because of the NONOates formation chemistry based on the deprotonation of amine groups through the sodium methoxide catalyst promoting the nucleophilic attack on nitric oxide[39], the transformation from amine and amide group to NONOates may have occurred at the interfaces between the solution dissolving sodium methoxide and the films. Thus, the porous, rough structure with the proportionally increased surface area might induce the proportional increase of NO donor to film growth.

Figure 3 showed the UV-vis absorbance graph comparing before and after NO donor synthesis. Based on previous studies, the NONOates has its specific absorbance peak at the 252 nm wavelength[11,42]. As shown in Fig. 3a, there were specific peaks for TA at 220 and 276 nm[43,44] and for Gel at approximately 190 nm (normal protein peak). These results correspond to the UV absorbance peak of the Gel and TA solution. (see Supplementary Fig. 1) However, after 3 days of the NONOates synthesis reaction, a specific peak for the NO donor was observed at 252 nm (Fig. 3b). Thus, we confirmed the NONOates was successfully generated in the films. Figure 3c shows the difference in absorbance intensity after the HPR. The peak showed that the amount of NONOates increased proportionally with the

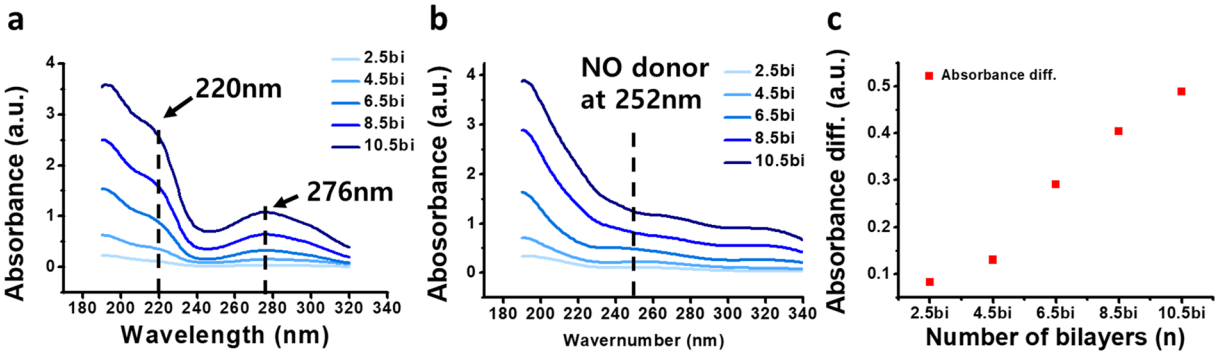

Figure 3. Analysis of nitric oxide donor formation via UV-vis absorbance measurement. (**a**) Absorbance graph before high pressure reaction and (**b**) NO donor peak at 252 nm after high pressure reaction. Absorbance difference for comparing before and after high pressure reaction is depicted in (**c**).

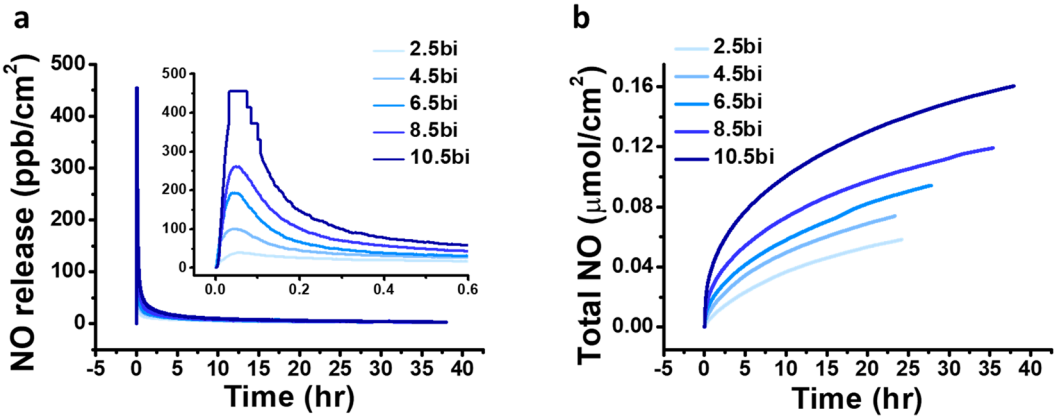

Figure 4. (**a**) Real-time NO release profile measured by nitric oxide analyzer and inset graph showed different time region. (**b**) Accumulated NO release amount depends on the number of bilayers.

thickness. The gradual increasing tendency of peak differences following the number of bilayers increased consistently with the increase in roughness (Fig. 2 roughness table). Consequently, we concluded that as the film grew, the roughness of the films is increased and it affected the amount of NO donor in the film. Therefore, by controlling film roughness and thickness, the loading amount of the NO donor in the film can be controlled.

NO release profiles. Based on this perspective, we analyzed and compared a NO release profile of each film to confirm the correlation between film morphology and NO release control. As the NONOates release NO gas instantly and continuously being triggered by proton, the release profile depends on its hydrated surface area. Because the porous and rough film structure has a higher surface area to volume ratio than a flat surface, they will have higher NO gas release per unit time and area when immersed into the physiological conditions. We evaluated the correlation between film morphology and NO release based on the amount of NONOates quantified from the UV results. We analyzed NO release from each film under mimicked physiological conditions (PBS, pH 7.4, 37 °C). Figure 4 shows the real-time NO release and accumulated NO amount. The $(gel/TA)_{10.5}$ film reached the maximum NO release (454.5 ppb/cm^2, see Table 1) in 2 min, and the half-life of the total amount released was approximately 5.5 h. Considering that the total duration of NO release was 38.0 h, half of the total NO was released from the film in 15% of the total duration time. It means the $(Gel/TA)_n$ film has very burst release profile, confirming the correlation between the surface roughness and NO release profile. The $(gel/TA)_{2.5}$ film showed maximum NO release of 38.8 ppb/cm^2 in 3.8 min to reach it. The $(gel/TA)_{6.5}$ film showed maximum NO release of 193.2 ppb/cm^2 in 2.7 min to reach it as shown in Table 1. Thus, as film roughness and thickness increased, the maximum amount of NO flux exponentially increased and time consumed for reaching the maximum decreased. The time required to reach the maximum decreased in an inverse proportion from 2.5 to 10.5 bilayers. This can be explained based on previous results and our hypothesis. Increased film roughness produced a larger surface area which could generate more NO donor moieties in the film structure (Fig. 3). Subsequently, the increased film roughness generated NO gas immediately from the interface between the film and PBS solution, resulting in a burst release profile. Considering the fact that NONOates is a proton-responsive NO donor and spontaneously generated NO, the burst release was occurred from the increased surface area to react with protons. Additionally, the total amount of NO released can be controlled depending on the film thickness. As shown in Fig. 4b and

$(Gel/TA)_n$ film	Total NO ($nmol \cdot cm^{-2}$)	$t_{1/2}$ (hr)	$[NO]_m$ ($ppb \cdot cm^{-2}$)	t_m (min)	t_d (hr)
2.5bi	58.4	6.99	38.8	3.8	24.2
4.5bi	73.9	5.69	100.0	2.8	23.4
6.5bi	94.4	6.52	193.2	2.7	27.8
8.5bi	119.2	6.25	261.8	2.8	35.4
10.5bi	160.5	5.56	454.5	2.0	38.0

Table 1. Summary of NO release profile depending on the number of bilayers. Total NO: total NO release amount, $t_{1/2}$: half-life of NO release profile, $[NO]_m$: maximum NO flux, t_m: the time consumed to reach the maximum NO flux, t_d: the duration time of total NO release.

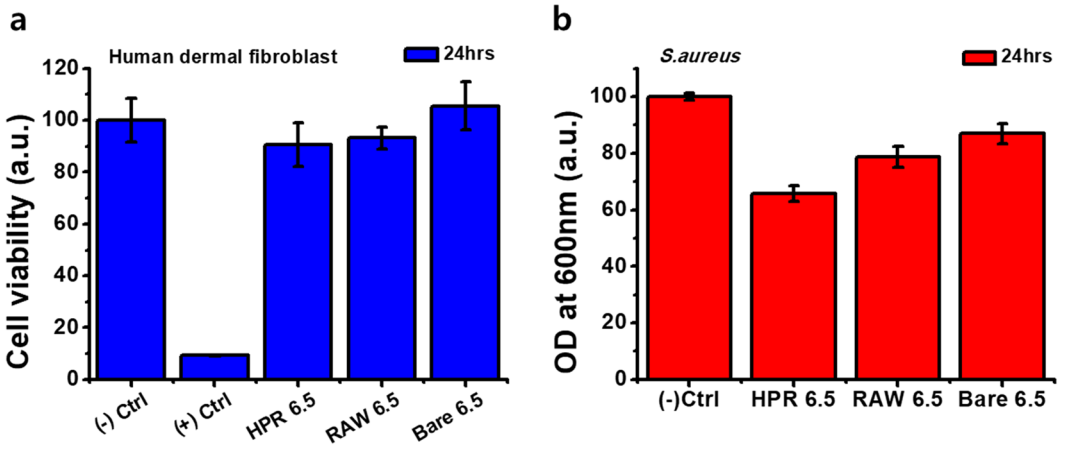

Figure 5. Cytotoxicity test for human dermal fibroblast and anti-bacterial effect against Staphylococcus aureus of $(Gel/TA)_{6.5}$ film. (**a**) Cell viability and (**b**) Bacterial density measured by optical density after treating the sample for 24 h.

Table 1, the total NO released from each film varied from 58.4 to 160.5 $nmol/cm^2$. According to the NO release data showing that thicker films generated more NO gas, NO release can be adjusted using the $(Gel/TA)_n$ film system. In addition, the film showed burst release in the beginning which can be applied for antibacterial coating but also have long release duration and nano-molar range of NO flux that can be applied for promoting cell signaling. Therefore, this the $(Gel/TA)_n$ system can be a good suggestion to design a NO release coating for biomedical purpose because of their controllable ability and inherent biocompatibilities of its composition materials.

Film toxicity and antibacterial effect. To apply this film in biomedical devices and applications, the toxicity test of the film must have preceded. The $(Gel/TA)_{6.5}$ film was used to observe the effects on the human dermal fibroblast (HDF) cells. We prepared three films to investigate the toxicity of NO gas released from the film: bare wafer (BARE 6.5), before high-pressure reaction film (RAW 6.5), and after high-pressure reaction (HPR 6.5) (Fig. 5a). We measured the viability of HDF cells after 1 day of film treatment by MTT assay. The HPR 6.5 sample showed 90% cell viability compared to the negative control group. The RAW 6.5 sample showed 93.2% viability, and thus the NO gas released from HPR 6.5 was not toxic towards HDF cells. Therefore, considering the 420 nm thickness and 94.4 nM of NO release of $(Gel/TA)_{6.5}$ film, this can be applied as a nano-thickness coating such as stent coating for vasodilation or particle coating for cell proliferation[10,45].

As one of the most widely studied applications of NO in biomedical applications, the antimicrobial effects of nitric oxide have been demonstrated through previous works[10]. Especially, *Staphylococcus aureus*, a common Gram-positive pathogen, has been used as the target bacteria because of its significance that it is the leading cause of skin and soft tissue infections[32,46,47]. The mechanism of the bactericidal effects of NO has arisen from the nitrosative and oxidative species produced by the reaction of NO with oxygen. The reaction produced reactive nitrogen species such as peroxynitrite, nitrogen dioxide, dinitrogen trioxide, and S-nitrosothiols[48]. These species can cause DNA damage, disrupt metabolic enzymes, and consequently induce bactericidal effects[49]. In this study, we evaluated the antibacterial effects of the $(Gel/TA)_{6.5}$ film against *S. aureus*. We measured the optical density to determine the bacteria density in the medium after immersing each film in a multi-well plate for 24 h. We compared the bare wafer (BARE 6.5), before high-pressure reaction film (RAW 6.5), and after high-pressure reaction (HPR 6.5) samples. As shown in Fig. 5b, the HPR 6.5 sample showed 35% decreased bacteria density compared to the negative control. This demonstrated that the $(Gel/TA)_{6.5}$ film has antibacterial effects. Thus, the $(Gel/TA)_n$ film can be applied as an effective NO delivery system for biomedical device coating and can prevent bacterial infections and cytotoxicity.

Conclusion

In this study, we developed a multilayer film for a NO gas delivery system by LbL assembly using nature obtained biocompatible materials, gelatin and tannic acid. The film was successfully constructed with 544 nm for 6 bilayers and concisely achieved the different thickness by controlling the number of bilayers. It showed a very rough, porous structure increasing proportionally as film thickness increased. NO donor formation was analyzed by specific UV absorbance peak of NONOates. We verified that the amount of NO donors incorporated in the film is coinciding with the roughness data because the donor formation reaction occurred at the interface of film and the catalyst dissolving solution. The amount of NO released was correlated with the increase in film roughness and the rough film showed rapid and burst release profile. We evaluated the $(Gel/TA)_n$ film system's potential in biomedical applications via cell viability testing using HDF cells and antibacterial test against *S. aureus* with $(Gel/TA)_{6.5}$ film. The $(Gel/TA)_{6.5}$ film revealed 90% cell viability and 35% decreased bacteria. In conclusion, the $(Gel/TA)_n$ polymeric films can be used as a novel NO-releasing coating system with a controlled release profile and high biocompatibility.

Materials and Methods

Materials. Gel from porcine skin (type A, gel strength 300), tannic acid (TA), ethanol anhydrous, and methanol anhydrous were purchased from Sigma-Aldrich (St. Louis, MO, USA). Sodium methoxide was from Acros Organics (Geel, Belgium). Silicon wafers were obtained from Namkang Hitech Co., Ltd. (Gyunggi-Do, Korea) and used as substrates.

Solution preparation. We prepared Gel solution and TA solution at a concentration of 1 mg/mL, which is enough for thermodynamically driven film fabrication of polyelectrolytes[50]. To dissolve the Gel, we heated the Gel solution for 30 min at 60 °C after mixing the Gel powder in deionized water. Subsequently, we stirred the Gel solution for 30 min. We simply prepared the TA solution in deionized water by vigorous mixing for 30 min. The pH of each solution was adjusted using 0.1 and 0.5 M sodium hydroxide solutions. The pH of gelatin solution was 6.5 and that of the TA solution was 7.0.

Multilayer film fabrication. We used simple immersive method dipping the silicon wafer in polymer solution as described previously[18]. First, the silicon wafer was oxidized with an oxygen plasma treatment machine (CUTE-1B, Femto Science, Somerset, NJ, USA) for cleaning and functionalizing the surface. Next, we dipped the silicon wafer into Gel solution for 10 min followed by rinsing twice for 2 min with pH 6.5 deionized water. The wafer was dipped into TA solution for 10 min followed by rinsing twice with pH 7.0 deionized water for 2 min each. This is the one bilayer fabrication step. We repeated the fabrication steps until achieving films of different thicknesses and we compared their surface morphology and roughness.

Film characterization. The thickness of the Gel/TA multilayer film was measured with a profilometer (Dektak 150, Veeco, Plainview, NY, USA). The surface morphology of the multilayer film was analyzed by FE-SEM (Carl Zeiss, Oberkochen, Germany). Topographic imaging and root-mean-square roughness measurements were conducted by AFM (NX10, Park Systems, Suwon, Korea). We confirmed *N*-diazeniumdiolate (NO donor) formation in the Gel/TA film by UV-vis (Evolution 300, Thermo Scientific, Waltham, MA, USA).

***N*-Diazeniumdiolate synthesis into the Gel/TA multilayer film by high-pressure reaction of NO gas.** We synthesized *N*-diazeniumdiolates (NONOates) in the Gel/TA multilayer film through a high-pressure reaction (HPR) using NO gas modified previous paper[51]. We prepared anhydrous ethanol and methanol at a 4:1 ratio in a 40-mL vial. We added enough solution to immerse the film. Next, 22.2 µL of sodium methoxide was added in the same molar amount as NONOate formation sites from 10 mg of gelatin. The solution was mixed by vortexing and the Gel/TA multilayer films were placed in a 40-mL glass vial and then placed in a high-pressure reactor (custom-made, Hanwoul Engineering Co., Ltd., Gyeonggi-do, Korea). We purged the reaction chamber with 10 atm of Ar gas after which the chamber was vented immediately. After three rapid purges, we purged the chamber for 10 min with 10 atm of Ar gas and removed the gas three times. The chamber was filled with 10 atm of NO gas and reacted for 3 days. We removed all gas and purged the chamber with 10 atm of Ar gas three times rapidly before removing the samples. The samples were rinsed with pure ethanol and dried under vacuum condition. All experiment process was carried out under room temperature.

NO release measurement. We analyzed the real-time NO release profile for the multilayer film using an NO analyzer (Sievers NOA 280i, GE Analytical Instruments, Little Chalfont, UK) in phosphate-buffered saline (PBS) at pH 7.4 and 37 °C. Ar gas was used as a carrier gas to move the generated NO gas. We measured the NO release profile to below 10 ppb.

Cell viability test. We investigated cell viability by the MTT (3-(4,5-dimethylthiazole-2-yl)-2,5-diphenyl tetrazoliumbromide, M2128, Sigma) assay. We seeded human dermal fibroblasts (HDF) into a 24-well plate with 1×10^4 cells in each well and cultured the cells in HDF growth medium (Dulbecco's Modified Eagle's Medium containing 10% vol fetal bovine serum and 1% vol penicillin-streptomycin) at 37 °C and 5% of CO_2 overnight ($n = 3$). After the cells adhered, the $(Gel/TA)_{6.5}$ film was placed in the wells and cultured for 24 h. The samples were then removed and the culture medium was replaced with a 10% MTT solution. After 2 h, the culture medium was removed and MTT formazan was dissolved by DMSO. The absorbance of each well was measured at 570 nm using a plate reader.

Antibacterial test. We purchased *Staphylococcus aureus* cells from the American Type Culture Collection (Manassas, VA, USA). *Staphylococcus aureus* was cultured in tryptic soy broth (soybean-casein digest media; BD

Biosciences, Franklin Lakes, NJ, USA) at 37 °C under aerobic conditions. We used bacterial strains at an optical density (OD, measured at 600 nm) of 0.58. We placed the $(Gel/TA)_{6.5}$ multilayer films (before (RAW 6.5) and after (HPR 6.5) and the bare silicon wafer (BARE) in a 24-well plate with tryptic soy broth medium and *S. aureus* for 24 h. Following the appropriate culture time, the wafers were removed. Next, we measured the OD at 600 nm with a plate reader to analyze bacterial growth.

References

1. Moncada, S. Nitric oxide: physiology, pathophysiology, and pharmacology. *Pharmacol rev* **43**, 109–142 (1991).
2. Beckman, J. S. & Koppenol, W. H. Nitric oxide, superoxide, and peroxynitrite: the good, the bad, and ugly. *American Journal of Physiology-Cell Physiology* **271**, C1424–C1437 (1996).
3. Murohara, T. *et al*. Nitric oxide synthase modulates angiogenesis in response to tissue ischemia. *The Journal of clinical investigation* **101**, 2567–2578 (1998).
4. Papapetropoulos, A., García-Cardeña, G., Madri, J. A. & Sessa, W. C. Nitric oxide production contributes to the angiogenic properties of vascular endothelial growth factor in human endothelial cells. *The Journal of clinical investigation* **100**, 3131–3139 (1997).
5. Ziche, M. *et al*. Nitric oxide mediates angiogenesis *in vivo* and endothelial cell growth and migration *in vitro* promoted by substance P. *The Journal of clinical investigation* **94**, 2036–2044 (1994).
6. Bogdan, C. Nitric oxide and the immune response. *Nature immunology* **2**, 907 (2001).
7. Lundberg, J. O., Weitzberg, E. & Gladwin, M. T. The nitrate–nitrite–nitric oxide pathway in physiology and therapeutics. *Nature reviews Drug discovery* **7**, 156 (2008).
8. Rajfer, J., Aronson, W. J., Bush, P. A., Dorey, F. J. & Ignarro, L. J. Nitric oxide as a mediator of relaxation of the corpus cavernosum in response to nonadrenergic, noncholinergic neurotransmission. *New England Journal of Medicine* **326**, 90–94 (1992).
9. Sanders, K. M. & Ward, S. M. Nitric oxide as a mediator of nonadrenergic noncholinergic neurotransmission. *American Journal of Physiology-Gastrointestinal and Liver Physiology* **262**, G379–G392 (1992).
10. Carpenter, A. W. & Schoenfisch, M. H. Nitric oxide release: Part II. Therapeutic applications. *Chemical Society Reviews* **41**, 3742–3752 (2012).
11. Hetrick, E. M. *et al*. Bactericidal efficacy of nitric oxide-releasing silica nanoparticles. *Acs Nano* **2**, 235–246 (2008).
12. Suchyta, D. J. & Schoenfisch, M. H. Controlled release of nitric oxide from liposomes. *ACS Biomaterials Science & Engineering* **3**, 2136–2143 (2017).
13. Reighard, K. P. *et al*. Role of nitric oxide-releasing chitosan oligosaccharides on mucus viscoelasticity. *ACS Biomaterials Science & Engineering* **3**, 1017–1026 (2017).
14. Kim, J., Saravanakumar, G., Choi, H. W., Park, D. & Kim, W. J. A platform for nitric oxide delivery. *Journal of Materials Chemistry B* **2**, 341–356 (2014).
15. Kim, J. *et al*. NONOates–polyethylenimine hydrogel for controlled nitric oxide release and cell proliferation modulation. *Bioconjugate chemistry* **22**, 1031–1038 (2011).
16. Ariga, K., Lvov, Y. M., Kawakami, K., Ji, Q. & Hill, J. P. Layer-by-layer self-assembled shells for drug delivery. *Advanced drug delivery reviews* **63**, 762–771 (2011).
17. Johnston, A. P., Cortez, C., Angelatos, A. S. & Caruso, F. Layer-by-layer engineered capsules and their applications. *Current Opinion in Colloid & Interface Science* **11**, 203–209 (2006).
18. Richardson, J. J., Björnmalm, M. & Caruso, F. Technology-driven layer-by-layer assembly of nanofilms. *Science* **348**, aaa2491 (2015).
19. Ji, Q. *et al*. Enhanced adsorption selectivity of aromatic vapors in carbon capsule film by control of surface surfactants on carbon capsule. *Bulletin of the Chemical Society of Japan* **91**, 391–397 (2017).
20. Zhang, D., Fan, X., Yang, A. & Zong, X. Hierarchical assembly of urchin-like alpha-iron oxide hollow microspheres and molybdenum disulphide nanosheets for ethanol gas sensing. *Journal of colloid and interface science* **523**, 217–225 (2018).
21. Shiratori, S. S. & Rubner, M. F. pH-dependent thickness behavior of sequentially adsorbed layers of weak polyelectrolytes. *Macromolecules* **33**, 4213–4219 (2000).
22. Li, Y., Wang, X. & Sun, J. Layer-by-layer assembly for rapid fabrication of thick polymeric films. *Chemical Society Reviews* **41**, 5998–6009 (2012).
23. Hong, J. *et al*. Graphene multilayers as gates for multi-week sequential release of proteins from surfaces. *Acs Nano* **6**, 81–88 (2011).
24. Fujimoto, K., Toyoda, T. & Fukui, Y. Preparation of bionanocapsules by the layer-by-layer deposition of polypeptides onto a liposome. *Macromolecules* **40**, 5122–5128 (2007).
25. Choi, D., Heo, J. & Hong, J. Controllable drug release from nano-layered hollow carrier by non-omnipresent enzyme in human condition. *Nanoscale* (2018).
26. Choi, M., Choi, D. & Hong, J. Multilayered controlled drug release silk fibroin nano-film by manipulating secondary structure. *Biomacromolecules* (2018).
27. Boulmedais, F. *et al*. Polyelectrolyte multilayer films with pegylated polypeptides as a new type of anti-microbial protection for biomaterials. *Biomaterials* **25**, 2003–2011 (2004).
28. Zhao, J. *et al*. Fabrication of ultrathin membrane via layer-by-layer self-assembly driven by hydrophobic interaction towards high separation performance. *ACS applied materials & interfaces* **5**, 13275–13283 (2013).
29. Shutava, T., Prouty, M., Kommireddy, D. & Lvov, Y. pH responsive decomposable layer-by-layer nanofilms and capsules on the basis of tannic acid. *Macromolecules* **38**, 2850–2858 (2005).
30. Aewsiri, T., Benjakul, S., Visessanguan, W., Wierenga, P. A. & Gruppen, H. Antioxidative activity and emulsifying properties of cuttlefish skin gelatin–tannic acid complex as influenced by types of interaction. *Innovative food science & emerging technologies* **11**, 712–720 (2010).
31. Shutava, T. G., Balkundi, S. S. & Lvov, Y. M. (−)-Epigallocatechin gallate/gelatin layer-by-layer assembled films and microcapsules. *Journal of colloid and interface science* **330**, 276–283 (2009).
32. Carpenter, A. W., Worley, B. V., Slomberg, D. L. & Schoenfisch, M. H. Dual action antimicrobials: nitric oxide release from quaternary ammonium-functionalized silica nanoparticles. *Biomacromolecules* **13**, 3334–3342 (2012).
33. Bjarnsholt, T. *et al*. Why chronic wounds will not heal: a novel hypothesis. *Wound repair and regeneration* **16**, 2–10 (2008).
34. Aramwit, P., Jaichawa, N., Ratanavaraporn, J. & Srichana, T. A comparative study of type A and type B gelatin nanoparticles as the controlled release carriers for different model compounds. *Materials Express* **5**, 241–248 (2015).
35. Jöbstl, E., O'Connell, J., Fairclough, J. P. A. & Williamson, M. P. Molecular model for astringency produced by polyphenol/protein interactions. *Biomacromolecules* **5**, 942–949 (2004).
36. Oh, H. I., Hoff, J. E., Armstrong, G. S. & Haff, L. A. Hydrophobic interaction in tannin-protein complexes. *Journal of Agricultural and Food Chemistry* **28**, 394–398 (1980).
37. Riedl, K. M. & Hagerman, A. E. Tannin− protein complexes as radical scavengers and radical sinks. *Journal of agricultural and food chemistry* **49**, 4917–4923 (2001).
38. Holland, R. J. *et al*. Direct Reaction of Amides with Nitric Oxide To Form Diazeniumdiolates. *The Journal of organic chemistry* **79**, 9389–9393 (2014).

39. Riccio, D. A. & Schoenfisch, M. H. Nitric oxide release: Part I. Macromolecular scaffolds. *Chemical Society Reviews* **41**, 3731–3741 (2012).
40. Hrabie, J. A. & Keefer, L. K. Chemistry of the nitric oxide-releasing diazeniumdiolate ("nitrosohydroxylamine") functional group and its oxygen-substituted derivatives. *Chemical reviews* **102**, 1135–1154 (2002).
41. Drago, R. S. & Karstetter, B. R. The reaction of nitrogen (II) oxide with various primary and secondary amines. *Journal of the American Chemical Society* **83**, 1819–1822 (1961).
42. Hrabie, J. A., Klose, J. R., Wink, D. A. & Keefer, L. K. New nitric oxide-releasing zwitterions derived from polyamines. *The Journal of Organic Chemistry* **58**, 1472–1476 (1993).
43. Liu, F. *et al*. Encapsulation of anticancer drug by hydrogen-bonded multilayers of tannic acid. *Soft matter* **10**, 9237–9247 (2014).
44. Katwa, L., Ramakrishna, M. & Rao, M. R. Spectrophotometric assay of immobilized tannase. *Journal of Biosciences* **3**, 135–142 (1981).
45. Napoli, C. *et al*. Effects of nitric oxide on cell proliferation: novel insights. *Journal of the American College of Cardiology* **62**, 89–95 (2013).
46. Lu, Y., Slomberg, D. L., Sun, B. & Schoenfisch, M. H. Shape-and Nitric Oxide Flux-Dependent Bactericidal Activity of Nitric Oxide-Releasing Silica Nanorods. *Small* **9**, 2189–2198 (2013).
47. Sun, B., Slomberg, D. L., Chudasama, S. L., Lu, Y. & Schoenfisch, M. H. Nitric oxide-releasing dendrimers as antibacterial agents. *Biomacromolecules* **13**, 3343–3354 (2012).
48. Jones, M. L., Ganopolsky, J. G., Labbé, A., Wahl, C. & Prakash, S. Antimicrobial properties of nitric oxide and its application in antimicrobial formulations and medical devices. *Applied microbiology and biotechnology* **88**, 401–407 (2010).
49. Grosser, M. R., Weiss, A., Shaw, L. N. & Richardson, A. R. Regulatory requirements for Staphylococcus aureus nitric oxide resistance. *Journal of bacteriology*, JB. 00229–00216 (2016).
50. Park, K., Choi, D. & Hong, J. Nanostructured polymer thin films fabricated with brush-based layer-by-layer self-assembly for site-selective construction and drug release. *Scientific reports* **8**, 3365 (2018).
51. Carpenter, A. W., Slomberg, D. L., Rao, K. S. & Schoenfisch, M. H. Influence of scaffold size on bactericidal activity of nitric oxide-releasing silica nanoparticles. *ACS nano* **5**, 7235–7244 (2011).

Acknowledgements

This research was supported by Basic Science Research Program through the National Research Foundation of Korea (NRF) funded by the Ministry of Science and ICT (NRF-2017R1E1A1A01074343). This research was supported by a grant of the Korea Health Technology R&D Project through the Korea Health Industry Development Institute (KHIDI), funded by the Ministry of Health & Welfare, Republic of Korea (Grant Number: HI15C1653).

Author Contributions

Designing the concept of the research: J.H., H.J, J.T, J.Y. and K.P. Performed experiments, analyzed the results and drawing scheme: K.P. Interpreted the data and wrote the manuscript: K.P. and and H.J. All authors reviewed and approved the final version of the manuscript for submission with approval of J.H.

Additional Information

Supplementary information accompanies this paper at https://doi.org/10.1038/s41598-019-44678-2.

Competing Interests: The authors declare no competing interests.

Publisher's note: Springer Nature remains neutral with regard to jurisdictional claims in published maps and institutional affiliations.